Original Article

Detection of Specular Reflection from Smart Colposcopy Image using RGB Color Space and Convolutional Neural Network

M. B. Jennyfer Susan[1], P. Subashini[2], M. Krishnaveni[3], T. Indhumathi[4]

[1,2,3,4]*Department of Computer Science, Centre for Machine Learning and Intelligence, Avinashilinam Institute for Home Science and Higher Education for Women, Tamil Nadu, India.*

[1]*Corresponding Author : 19phcsf008@avinuty.ac.in*

Abstract - Cervical cancer is a prevalent malignancy among women, particularly in developing nations with high fatality rates. Screening for cervical cancer often involves the use of smart colposcopy, which captures images of the cervix. However, specular reflection frequently affects these images, resulting in bright pixels that obscure neoplasm on the cervical images. To address this issue, proposed an intensity-based threshold method on RGB color space to identify specular reflection in smart colposcopy images. The binary masks are generated using this threshold, with glare regions represented as 1 and non-glare regions as 0, allowing for automated identification of specular reflection using convolutional neural networks such as the fully convolutional network and the U-Net Model. The proposed approach achieved an accuracy of 89.26% in identifying specular reflection using the threshold method alone. However, the combination of novel binary masking along with U-Net improved the accuracy to 99.71%. This study demonstrates the potential for the proposed method to improve the accuracy of identifying specular reflection in smart colposcopy images, which could ultimately enhance screening for cervical cancer in resource-limited settings.

Keywords - Cervical cancer, Specular reflection, Smart colposcopy image, Convolution Neural Network, RGB color space.

1. Introduction

Cervical cancer poses a significant global health challenge and ranks fourth most common cancer among women worldwide. Developing countries in Asia and Africa report a higher incidence of cervical cancer due to a lack of awareness and knowledge about the disease. For instance, in India alone, 96,922 new cases and 60,078 deaths were reported in 2020 due to cervical cancer [1]. The primary cause of cervical cancer is the Human papillomavirus (HPV), primarily transmitted through sexual contact. Early detection through regular screening programs can play a crucial role in preventing the disease, and it is often curable when identified at an early stage [2, 3].To aid in cervical cancer screening, MobileODT has introduced a digital smart colposcopy device capable of capturing images for analysis to identify abnormalities in the cervical regions [4]. However, during the visual analysis of these images, certain portions are often affected by bright white pixels known as specular reflection. Specular reflections are caused by the moisture content of tissue bodies, which absorb light from the surroundings and reflect as bright white pixels. These reflections can significantly impact the quality of the captured cervical images, making it challenging for physicians to analyze them accurately. Hence, detecting and eliminating specular reflection in the images is crucial to enhance their quality and make it easier for medical experts to conduct thorough analyses.

One such approach is the Dichromatic Reflection Model (DRM), which aims to separate diffuse and specular reflections from the images. However, this method often fails to detect saturated specular pixels in smart colposcopy images, especially when dealing with similar color regions [5]. Another approach is the gradient-based method, which uses color space models to detect specular reflection pixels [6]. This study explored using different color space models, such as RGB, HSV, XYZ, YUV, and LAB, to detect reflection from the images [10, 11]. The G channel of the RGB color space is commonly employed for detecting specular reflection in medical images due to its high-intensity value [7, 12].
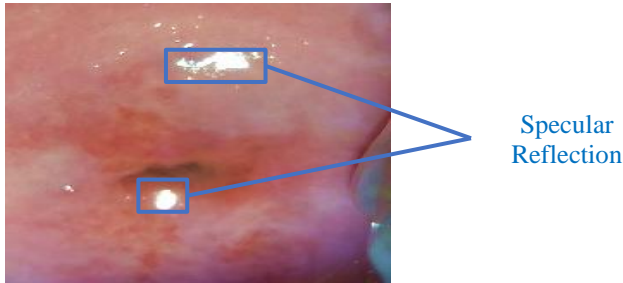
Fig. 1 Colposcopy image with specular reflection

Similarly, the HSV, XYZ, and LAB color space channels have been utilized for detecting specular reflection based on statistical operations and threshold methods [8, 9]

This paper introduces a novel method for detecting specular reflection in cervical images, specifically focusing on the threshold approach to avoid affecting non-specular pixels. The method involves analyzing the pixel values of each channel to identify the intensity value range associated with the reflection region. These identified regions are then labeled as the reflection region and used to train a convolutional neural network, which shows promising results in identifying the glare region. The structure of the paper is as follows: Section 2 presents an extensive examination of pertinent literature, discussing color space models commonly used for detecting specular reflection and convolutional neural network models applied in medical image segmentation. In Section 3, the conventional methods for specular reflection detection are presented, along with the challenges they face. The proposed method is then introduced as a solution to address these challenges effectively. Section 4 presents the experimental results and analysis of the proposed method, showcasing its performance in detecting specular reflection in cervical images. Finally, in Section 5, the paper concludes by summarizing the findings and the potential implications of the proposed method.

2. Literature Review

Specular reflection is a concern in Smart colposcopy images as it negatively impacts image quality. However, ensuring high-quality cervical images holds greater significance for physicians, as these images are crucial for analysis [13]. Various color space models have been employed to identify specular reflection in Smart colposcopy images and other medical visuals. This is because certain color channels within these models possess enhanced capabilities in spotting reflection in medical imagery, particularly in the case of cervical images. An algorithm is introduced to forecast the glare areas using standard deviation filters [7]. This approach serves as a pre-processing step subsequent to identifying and enhancing curvilinear structures in cervical images to facilitate cervix region segmentation. The algorithm extracts color channels recognized for their high-intensity values within the color space model to pinpoint glare regions. These

extracted color channels are processed, applying standard deviation filters to foresee glare regions within colposcopy images. The algorithm is implemented across various cervix image stages, involving manual calculation of predicted glare regions based on grading.

Additionally, the algorithm's performance is evaluated under diverse illuminations using GIMP 2 software. In terms of comparative analysis, the proposed method achieves glare region prediction with a sensitivity rate of 0.809. Notably, the pre-processed images yield superior segmentation results compared to the unprocessed counterparts.

The crucial role of colposcopy is the early-stage detection of cervical lesions [9]. Physiological mucus within the tissue body leads to the emergence of glare regions, identifiable as bright pixels in images captured via colposcopy devices. These highlighted areas exhibit a certain resemblance to abnormal metaplasia epithelium, such as acetowhite or lesion regions. This similarity poses challenges during medical image processing tasks like lesion region segmentation and grading, as distinguishing between them becomes intricate due to their shared properties. To address this issue, the author proposed a threshold-based segmentation approach applied to color images. This method leverages non-linear filtering techniques to accurately normalize and predict specular reflections. The process involves determining color balancing ratios and window sizes combined with applying a median filter. This combined approach aids in effectively detecting subtle specular pixel points within colposcopy images, particularly in cases where the specular regions exhibit lower intensity. An issue of specular reflection in endoscopy, a realm of digital imaging utilized to visualize internal human body structures. Specular reflection in endoscopic images often stems from bright areas and intense lighting, impacting the efficacy of minimally invasive surgeries [14].

The authors introduced an automated method for identifying specular reflection using the intrinsic Image Layer Separation (IILS) technique to tackle this challenge. Their approach involves several steps, commencing with image normalization. Subsequently, high-gradient areas are extracted to facilitate the separation of specular reflection via the utilization of a color model. Following this, a patch-based approach is applied to construct the reflection region, thereby enhancing the quality of endoscopy images. This proposed method serves as a pre-processing technique, paving the way for further analysis of endoscopic images. While the method achieves an impressive 99% accuracy in predicting specular reflection, it does encounter limitations when dealing with larger specular reflection regions within digital images.

A novel technique is introduced involving the formulation of a criterion to identify specular highlights on a per-pixel basis [21]. This criterion relies on assessing the red channel value relative to both the green and blue channel

values, providing an effective means of detecting specular highlights. The method capitalizes on image segmentation and introduces an adaptive threshold derived from variations between the red channel value and the values of other channels in adjacent pixels. To substantiate their approach, the researchers carried out experiments using clinical data and the CVC-ClinicSpec open database. The outcomes of these experiments illustrate the method's remarkable performance, achieving an average Precision of 88.76%, an Accuracy of 99.60%, and an F1-score of 72.56%. Notably, the proposed method surpasses the capabilities of existing state-of-the-art techniques grounded in color distribution and previously applied to endoscopic highlight detection. The author proposed an approach aimed at enhancing the diagnostic accuracy of endoscopic images by mitigating specular reflections [22].

This method employs supervised learning to identify and isolate highlights, subsequently restoring images by extending similar structural attributes from non-specular areas to the specular regions. A multiscale dynamic image expansion and fusion technique is employed to restore highlighted segments in endoscopic imaging. Separating specular reflections involves a combination of statistical thresholding and Support Vector Machine (SVM) learning, enabling an automated reflection separation process.

Candidate blocks are selected to replenish the empty regions with comparable content by addressing the voids left after reflection removal. The model is trained using a dataset of 55 images featuring specular spots. These images were sourced from ColonDB, which contains annotated video sequences of colonoscopy procedures. The proposed method's effectiveness is evaluated by measuring the predicted inpainted image, yielding a COV (Coefficient of Variance) value of 0.3168.

In conclusion, the collective insights from the reviewed studies underscore the pivotal role of addressing specular reflection in medical imaging, particularly in domains like cervical cancer screening and colposcopy. These research endeavors have revealed various methodologies and techniques that contribute to enhancing image quality, diagnostic accuracy, and subsequent medical analysis. So, this reflection on medical images is represented as the major problem in affecting the quality of the images, especially in the smart colposcopy images. So, to address these challenges proposed, the reflection detection process will be further discussed in the next sessions.

3. Methodology

The method under consideration employs the RGB color space to detect reflections in smart colposcopy images. A binary mask is formulated through the application of a threshold to these images, facilitating the extraction of this

mask. Subsequently, a model is trained using both the unaltered images and the masked ones to predict instances of specular reflection present in the smart colposcopy images.

3.1. Proposed Threshold Method for the Identifying Glare Areas

This paper proposes an intensity-based threshold method for identifying specular reflections in smart colposcopy images. Specular reflections are characterized by their high-intensity values, ranging from 191 to 255 on a scale of 0 to 255, where 0 represents the darkest pixel, and 255 represents the brightest region. Each pixel's intensity value is analyzed to identify the specular reflection region, and those falling within the 191-255 range are classified as specular reflections. The intelligent colposcopy images employed in this research were sourced from the Kaggle and uniformly resized to 256x256 dimensions using a bicubic interpolation algorithm [18]. Bicubic interpolation is particularly well-suited for medical images, as it maintains superior pixel quality compared to alternative interpolation methods. This resizing procedure was integrated into the masking process, guaranteeing uniform image size across all samples and facilitating their utilization in deep learning models. Each pixel's intensity value is compared to a threshold of 191 to detect the specular reflection region. If the pixel's intensity value is greater than or equal to 191, its value is set to 0, indicating the presence of a specular reflection. If the intensity value is less than or equal to 191, its value is set to 255, indicating the absence of a specular reflection. Algorithm 1 summarizes the process of detecting glare regions in smart colposcopy images.

Algorithm 1:

Input: Image Dataset represented as a 2D array "pixel" with size (img_height, img_width)
 	
For each x in range 0 to (img_height - 1)
  For each y in range 0 to (img_width - 1)
Set current_pixel = value of "pixel" at position (y, x)
    If current_pixel >= 190
      Set value of "pixel" at position (y, x) to 1
        Else if current_pixel <= 191
      Set the value of "pixel" at position (y, x) to 0
  End

Figure 2 illustrates the images where specular reflection has been detected using the method proposed in this study.
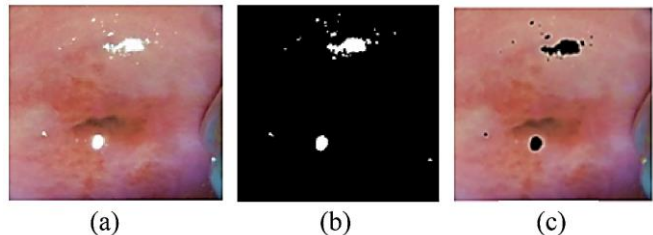

(a)   (b)   (c)

Fig. 2 Identification of Reflection on Colposcopy Images. (a) Original image (b) Proposed Binary Masking (c) Detected Reflection using Proposed Binary Masking

Figure 2 (a) depicts the source images with specular reflection on smart colposcopy images. Figure 2(c) represents the images with glare region detected with the proposed threshold method. Figure 2 (b) represents the masked image generated by the threshold method, which is used as ground truth for identifying the glare region.

3.2. Convolutional Neural Network for Identifying Glare Region on Colposcopy Images

Two segmentation models, called the fully convolutional neural network and the U-Net model, were employed to forecast specular reflection originating from cervical images[15, 16]. This predictive task is aimed at enhancing smart colposcopy images. This section elaborates on the input data, network architectures, as well as the training and testing processes. The dataset comprised 3582 colposcopy images featuring specular reflections, all sourced from the Kaggle dataset [23]. An innovative binary masking technique was introduced to label the specular reflection areas within these images. This method was then implemented across the entire set of 3582 images, yielding a collection of corresponding masked images. These masked images, alongside the original unaltered ones, were utilized as inputs for an advanced deep-learning model. The model's primary objective was to predict and delineate specular reflection occurrences in smart colposcopy images.

3.2.1. Fully Convolutional Network (FCN)

The Fully Convolutional Network (FCN) is an advanced extension of the feed-forward neural network, primarily designed to effectively segment digital images [20]. Its structure is composed of two key components: the encoder network and the decoder network. The Encoder network is constructed using the pre-trained VGG16 model, enabling the extraction of essential features from input images. In contrast, the decoder network conducts up-sampling of the feature maps, aiming to restore the dimensions of the encoded features to match the original input image size. Deconvolutional layers are employed for this purpose, ultimately generating a segmentation map.

The FCN integrates skip connections between the encoder and decoder networks to preserve intricate spatial details. These connections facilitate the amalgamation of lower-level features captured by the encoder with the higher-level features acquired by the decoder, culminating in a more precise segmentation map. The model's architecture encompasses 3x3 kernel sizes with a stride value 1. A dropout rate of 0.2 is implemented, and batch normalization is activated.

3.2.2. U-Net Model for Segmentation

The network architecture utilized in this study encompasses two principal components: a contracting path and an expansive path [17, 19]. The contracting path adheres to the conventional Convolutional Neural Network (CNN) structure, characterized by the iterative application of two unpadded 3x3 convolutional layers. Subsequent to each layer, a Rectified Linear Unit (ReLu) is applied, followed by a 2x2 max pooling operation with a stride of 2, facilitating downsampling. Throughout each downsampling stage, the count of feature channels doubles. Conversely, each phase within the expansive path commences with a feature map upscaling, succeeded by a 2x2 upconvolution that reduces the feature channel count by half.

The upsampled feature map is merged with the correspondingly cropped feature map from the contracting path. Following this, two 3x3 convolutions are executed, each followed by a ReLu activation. Cropping is implemented on the images to account for the border pixel loss during convolutions. A 1x1 convolution is applied in the final layer, mapping each 64-component feature vector to the desired class count. The complete network encompasses a total of 23 convolutional layers.

4. Training and Result Analysis

This section outlines the experimental configuration necessary for implementing the proposed model and subsequently examines the outcomes through both quantitative and qualitative analyses, comparing the conventional and the proposed methods. In preparation for training, the input images undergo resizing to dimensions of 256x256x3. The training dataset comprises 3,582 images of size (3582, 256, 256, 3), the testing dataset contains 448 images of size (448, 256, 256, 3), and the validation dataset includes 448 images of size (448, 256, 256, 3).

The U-Net model utilizes original and masked images as input for predicting specular reflection. Masked images play the role of labeling specular reflections to predict glare regions. A batch size of 32 and a learning rate of 0.001 are employed during training. The utilization of the Adam optimizer is preferred due to its computational efficiency and its capacity to manage noisy or sparse gradients that are often encountered in medical images. The binary cross-entropy loss function is adopted, while the activation function employed is sigmoid. Model training is executed for a total of 50 epochs.

4.1. Experimental Settings

The CNN models used for predicting specular reflection on cervical photos are trained using Smart colposcopy images sourced from the Kaggle dataset [23]. A pool of 6,734 smart colposcopy images is available initially, but 2,256 images are excluded due to noise, leaving 4,478 images for further analysis to identify glare regions.

This dataset is then divided into training, testing, and validation subsets in an 80%, 20%, and 20% ratio, respectively. A machine equipped with a Tesla V100 PCIe GPU and CUDA version 11.4 is employed for model training,

providing the necessary computational power to train the deep-learning models effectively and efficiently.

4.1.1. Identification of Suitable Threshold for Reflection Detection

Each and every pixel of the images is analyzed to identify the numerical value of the pixels that fall in the specular reflection region. Each pixel intensity range was analyzed to determine this range, and the results are displayed in Figure 3. Figure 3 (a) shows the original images with specular reflection. Figure 3 (b), the range value of 187-255 is used to predict the specular reflection. It shows some of the non-specular reflection is identified in this intensity range, as highlighted in the violet box. Figure 3(c) and (d) show the pixel intensity value ranges of 189-255 and 190-255, respectively, where the specular reflection region was identified along with the non-glare region, which affects image quality during further analysis. Finally, in Figure 3(e), the pixel value range of 191-255 was used to identify the glare region. Only specular reflections were identified through analysis without affecting the other non-specular reflections. In conclusion, the proposed method effectively identified specular reflection, and the pixel value range of 191-255 provided the most accurate detection of specular reflection without affecting the non-glare region.

4.1.2. Identification of Reflection Region Without Affecting the White Tissue Region

Another set of challenges arises during the process of identifying specular reflection, particularly concerning regions of white tissue in the images. Notably, the specular reflection range of 191-255 does not adversely impact image quality, nor does it interfere with depicting other components like white discharge and various tissue areas within cervical images, as demonstrated in Figure 4. The proposed method demonstrates accurate detection of specular reflection across all three categories of cervical images, encompassing CIN-1, CIN-2, and CIN-3. This effectiveness extends to datasets containing a substantial number of images for each type of cervical image, as detailed in Table 1. The dataset comprises three distinct cervical image types, namely CIN1, CIN2, and CIN3, each corresponding to different levels of cancer severity within the tissue region. In the context of cancer progression, CIN1 represents an early stage where approximately one-third of the tissue region is affected by cancer cells. As cancer advances, such as in CIN2 and CIN3, cancer cells' presence increases, particularly in the acetowhite region. Particularly challenging is the precise isolation of specular reflection from the acetowhite region in CIN3 cases due to the heightened complexity of the images at this stage. So, from the three types of cancer randomly selected, the 1000 images are selected from the three types of cervical images. The 250 images from CIN1, 250 images from CIN2 type, and 500 images from CIN3 are used to evaluate the detection of reflection from the cervical images without affecting the white tissue and acetowhite region.
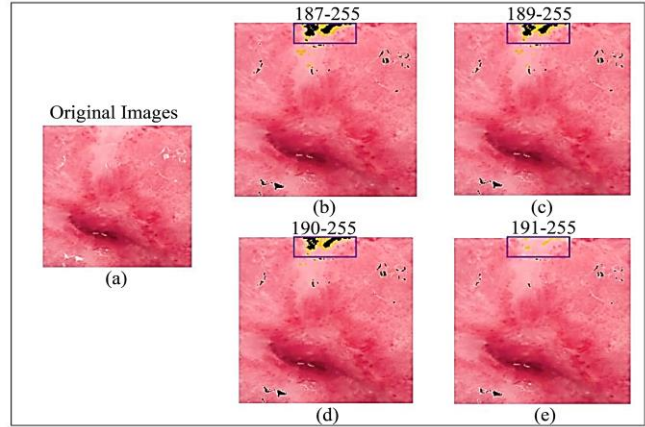
Fig. 3 Detection of specular reflection on each pixel intensity value
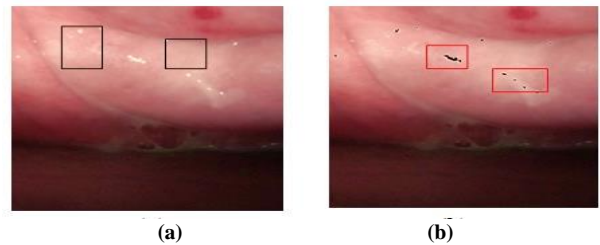
Fig. 4 Reflection detected without influencing the white region. (a) Original Images with Specular Reflection and white tissue region masked in the black box. (b)Specular reflection was detected and marked in a red box without affecting the white tissue region.

4.1.3. Comparison Method

For comparison analysis, three existing model used for identifying reflection using the threshold method on different color space is used in this paper.
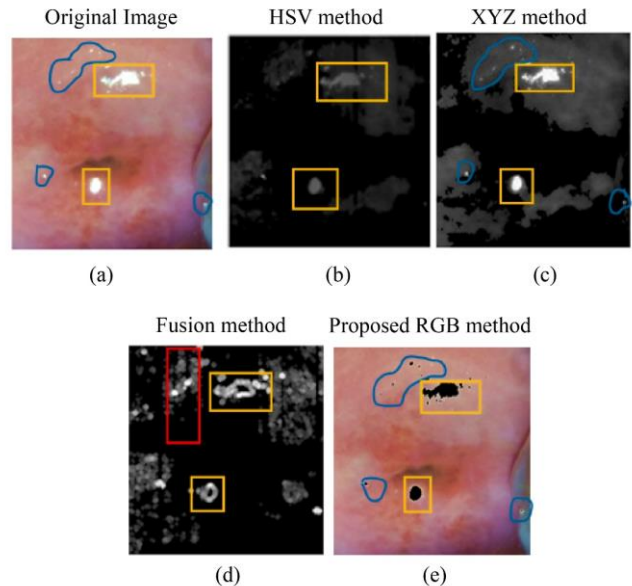

Fig. 5 Qualitative Analysis of the conventional and the proposed RGB method. Red represents the non-specular region identified as the specular region. Blue represents the small-scale intensity value of the specular region, and yellow represents the identified large-scale intensity value

Table 1. Specular reflection detection analysis on each type of cervix images

Methodology	CIN-1 (250 Images)	CIN-2 (250 Images)	CIN-3 (500 Images)
HSV [14]	170	85	251
XYZ [8]	148	154	369
Fusion [7]	94	96	116
Proposed RGB	222	232	473

On analyzing the HSV color space method, the cervical images' pixels were damaged, and the non-specular regions were removed, as shown in Figure 5 (b). Although specular reflection was identified, it is unclear whether it identified the small specular reflection regions on the cervical images. As a result, this approach negatively impacted the cervical image quality, making it difficult to conduct further analysis. On the other hand, the XYZ method identified both large and small intensity regions of the specular reflection. However, the color of the cervical images was affected, and it was impossible to convert them back to color images, as shown in Figure 5(c). Since the color of the cervical images is crucial for further analysis, this approach's limitation reduces its effectiveness. The fusion method is the combination of three color spaces. The glare region identified is not clear as it appears as the dotted region, as shown in Figure 5 (d). The proposed method identifies the specular reflection of the cervical images' small-scale and large-scale intensity regions, as shown in Figure 5 (e). The color of the cervical images is non-affected and helps further analysis and processing. The comparison of the proposed RGB method and the convention method images are displayed in Table. 2.

Based on the quantitative analysis, the proposed method predicts the specular reflection from cervical cancer with an accuracy of 89.26%, as shown in Table 3.

Table 2. Comparison analyses of the proposed and the conventional method
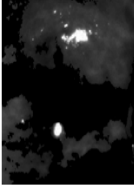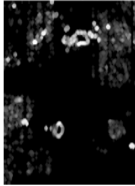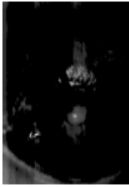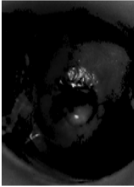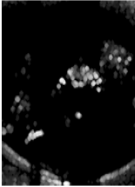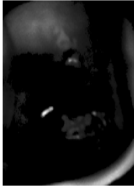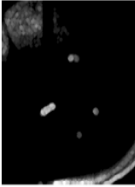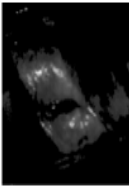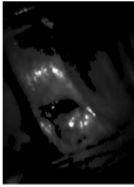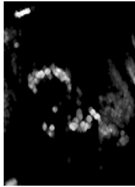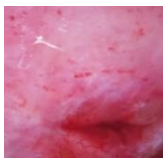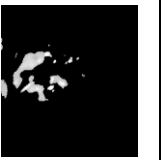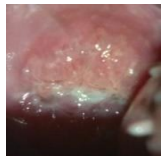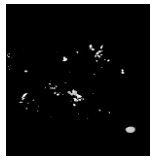
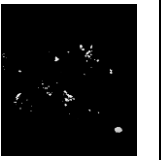| Original image	Proposed RGB Method	Conventional Method		
		HSV Method	XYZ method	Fusion Method

Table 3. Comparison analysis of the proposed RGB method with the conventional method

Methods	Accuracy (%)	Specificity (%)	Sensitivity (%)	Precision (%)
Proposed method	89.26	88.24	87.23	77.52
HSV [14]	85.03	83.14	82.74	75.36
XYZ [8]	82.39	80.02	81.72	72.35
Fusion method [7]	74.78	61.35	60.35	72.36

Table 4. Comparison analysis of the FCN and U-Net model for the identification of specular reflection. The red represents the non-specular region identified, and the yellow represents the specular reflection identified on the cervical images

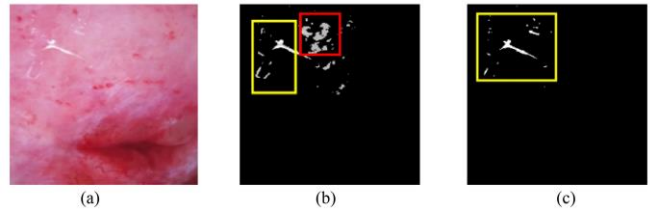| Original Image	Predicted Images	
	Proposed RGB method with FCN	Proposed RGB method with U-Net

Fig. 6 Comparison analysis of the FCN and U-Net model for the detecting reflections. Red represents the non-specular region identified, and yellow represents the reflection identified on cervical images
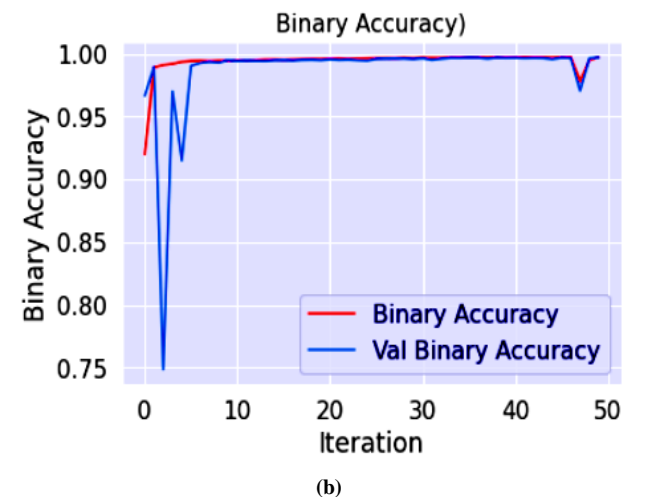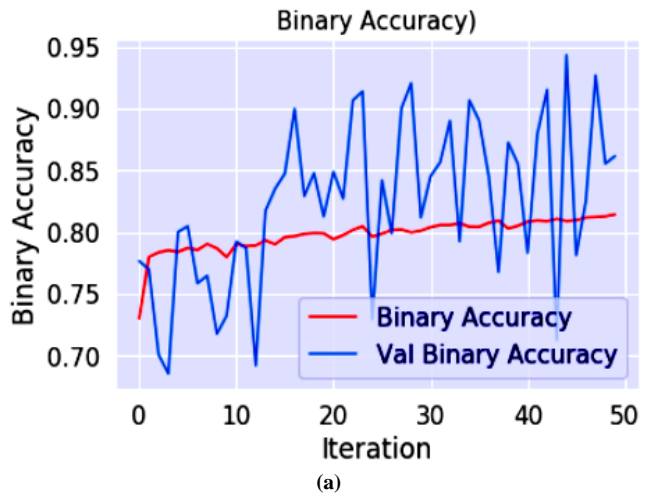

(a)

(b)

Fig. 7 Binary Accuracy for identifying glare region (a) Binary accuracy of FCN model. (b) Binary accuracy of U-Net model

4.1.4. Proposed Binary Masking along with Convolutional Neural Network for reflection identification

Utilizing binary masked images alongside the original images, the deep learning models—specifically the fully convolutional network and U-Net model—are employed for the purpose of reflection prediction. Subsequently, the forecasted specular reflection is subjected to both quantitative and qualitative analyses, focusing on its performance within the context of smart colposcopy images. The U-Net model outperforms other deep learning techniques in conducting a qualitative evaluation in accurately detecting specular reflection. Figure 6(a) illustrates that original images containing specular reflection are obtained from the Kaggle dataset. The application of the FCN model reveals the detected specular reflection, as depicted in Figure 6(b). Through analysis, it's apparent that specular reflection detection sometimes misinterprets non-specular regions as glare regions in smart colposcopy images. In contrast, Figure 6(c) showcases the outcome of detecting specular reflection employing the U-Net model. Notably, the U-Net model successfully identifies specular reflection without causing disruptions to other regions within the colposcopy images. This outcome is substantiated through thorough analysis, attesting to the U-Net model's precision in isolating specular reflection regions. The prediction of glare using the proposed along with the CNN models is depicted in Table 4.

For comparison, analysis of three existing models used for the prediction of specular reflection using the threshold method on different color spaces is used in this paper.

The binary accuracy, Union of Intersection (UoI), Dice Coefficient, and loss value are calculated for the quantitative analysis. This metric measures the percentage of correctly classified instances in a binary classification problem, where the output can only be one of two possible classes (e.g., 0 or 1, true or false, etc.).

Table 5. Comparison of proposed RGB method with the deep learning CNN models

Methods	Binary Accuracy	UoI	Dice Coefficient	Loss
RGB with FCN	0.8246	0.7984	0.8417	0.2017
RGB with U-Net	0.9973	0.8012	0.8679	0.1312

Based on the quantitative analysis, reflection is predicted with an accuracy of 99.73% in the U-Net convolutional model, as shown in Table 5. The binary accuracy, loss, and UoI for detecting reflection at each epoch are depicted in the figure 7, 8, and 9 respectively.

The deep-learning CNN models were trained for 50 epochs each. In the case of the FCN model, it achieved an accuracy of 82.46% in predicting glare regions by the 47th epoch. However, this model suffered from overfitting due to the limited size of the dataset, as evident from Figure 7(a). On the other hand, the UNet model managed to predict glare regions with an impressive accuracy of 99.73% at a mere 6 epochs, as shown in Figure 7(b). Importantly, this model exhibited no signs of overfitting.

Regarding the Union of Intersection (UoI) metric, the FCN model's performance was less stable, leading to fluctuating predictions with an UoI of 0.79, coupled with overfitting, as depicted in Figure 8(a). Contrastingly, the UNet model achieved an UoI of 0.80 without encountering overfitting concerns within 6 epochs.

The deep-learning CNN models were trained for 50 epochs each. In the case of the FCN model, it achieved a loss value of 0.20 in predicting glare regions by the 50th epoch. However, this model suffered from overfitting due to the limited size of the dataset, as evident from Figure 9(a). On the other hand, the UNet model managed to predict glare regions with a loss of 1.31 at a mere 47 epochs.
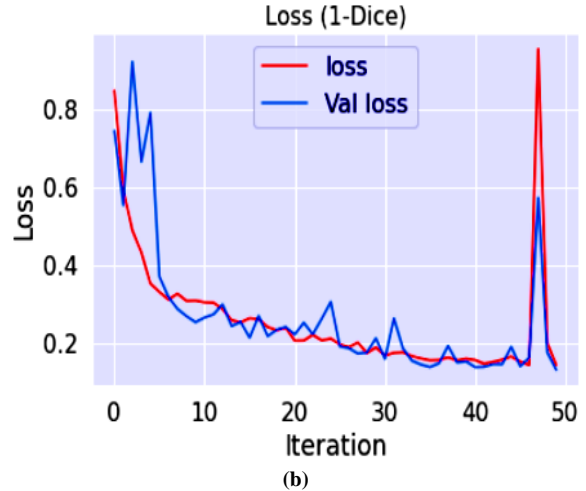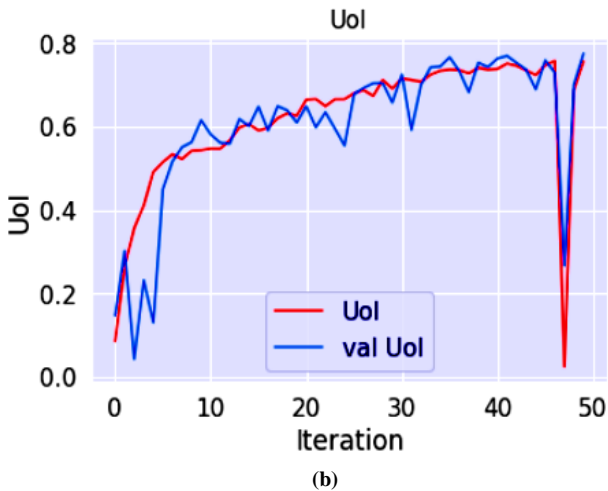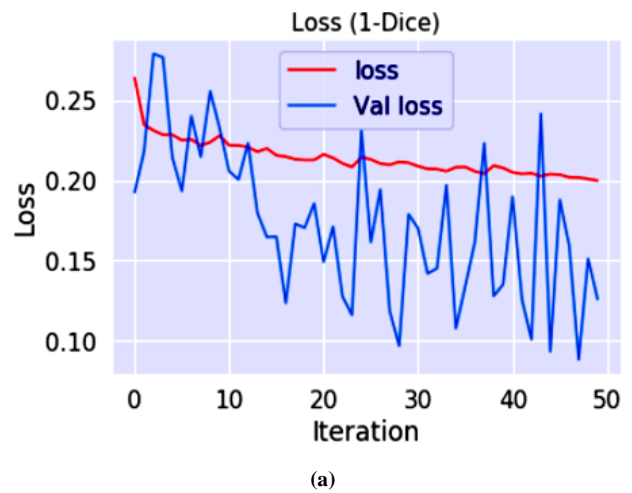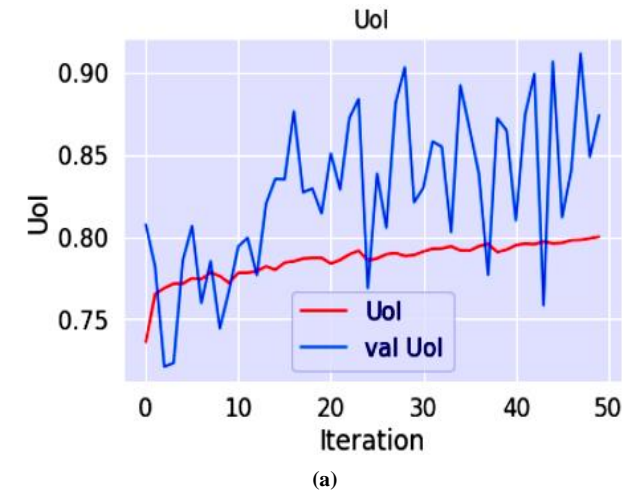

Fig. 8 Union of Intersection for prediction of glare region. (a) Union of Intersection of FCN model. (b) Union of Intersection of U-Net model

Fig. 9 Loss for predicting glare region (a) Loss of FCN model. (b) Loss of U-Net model

Table 6. GPU Processor for the training CNN Model

Model	Time execution/minutes	Memory Space/GB
U-Net	6 hours 23 minutes	15.86
FCN	7 hours 15 minutes	16.87

Based on the data presented in Table 6, the U-Net model's training, utilizing a memory space of 15.86 GB, requires approximately 6 hours and 23 minutes for specular reflection prediction from smart colposcopy images when utilizing GPU processing. On the other hand, the FCN model, which predicts glare regions, utilizes a memory of 16.87 GB and completes its execution in approximately 7 hours and 15 minutes.

5. Conclusion

In this paper, conventional methods for detecting specular reflection in medical images have been analyzed using three different colour spaces in the context of cervix images. However, these methods have certain limitations in accurately detecting specular reflection, particularly on small-scale regions, and they need to be automated, which makes them impractical for large-scale analysis. The paper proposes a computerized procedure that accurately detects specular reflection in cervix images to address these limitations. The proposed method has been evaluated quantitatively and qualitatively, and the results show that it outperforms conventional methods in accuracy. The detection process is based on intensity values, but one limitation of the proposed method is that it may not work well with images of varying illumination. Therefore, the paper suggests that future work should focus on predicting the glare region with an adaptive threshold based on image illumination, which could improve the accuracy of the proposed method.

Acknowledgments

References

[1] Ganesh Balasubramaniam et al., "Survival Rate of Cervical Cancer from A Study Conducted in India," *Indian Journal of Medical Sciences*, vol. 72, no. 1, pp. 203-211, 2020. [CrossRef] [Google Scholar] [Publisher Link]

[2] Cervical Cancer, 2022. [Online]. Available: https://www.who.int/health-topics/cervical-cancer#tab=tab_1

[3] C.O. Iloghalu et al., "An Intelligent Model for Improved Breast Cancer Prognosis," *SSRG International Journal of Electronics and Communication Engineering*, vol. 10, no. 8, pp. 36-47, 2023. [CrossRef] [Publisher Link]

[4] Rengaswamy Sankaranarayanan et al., "Visual Inspection of the Uterine Cervix After the Application of Acetic Acid in the Detection of Cervical Carcinoma and Its Precursors," *Cancer*, vol. 83, no. 10, pp. 2150-2156, 1998. [CrossRef] [Google Scholar] [Publisher Link]

[5] Steven A. Shafer, "Using Color to Separate Reflection Components," Color *Research and Application*, vol. 10, no. 4, pp. 210-218, 1985. [CrossRef] [Google Scholar] [Publisher Link]

[6] T.Gevers, and H.M. Stokman, "Classifying Color Transitions Into Shadow-Geometry, Illumination, Highlight or Material Edges," *International Conference on Image Processing*, vol. 1, pp. 521-524, 2000. [CrossRef] [Google Scholar] [Publisher Link]

[7] V. Kudva, K. Prasad, and S. Guruvare, "Detection of Specular Reflection and Segmentation of Cervix Region in Uterine Cervix Images for Cervical Cancer Screening," *Intermediate-Range Ballistic Missile*, vol. 38, no. 5, pp. 281-291, 2017. [CrossRef] [Google Scholar] [Publisher Link]

[8] Othmane El Meslouhi et al., "Automatic Detection and Inpainting of Specular Reflections for Colposcopic Images," *Open Computer Science*, vol. 1, pp. 341-354, 2011. [CrossRef] [Google Scholar] [Publisher Link]

[9] Xiaoxia Wang et al., "Detection and Inpainting of Specular Reflection in Colposcopic Images with Exemplar-Based Method," *13th International Conference on Anti-Counterfeiting, Security, and Identification*, pp. 90-94, 2019. [CrossRef] [Google Scholar] [Publisher Link]

[10] Abhishek Das, Avijit Kar, and Debasis Bhattacharyya, "Elimination of Specular Reflection and Identification of ROI: The First Step in Automated Detection of Cervical Cancer Using Digital Colposcopy," *IEEE International Conference on Imaging Systems and Techniques*, pp. 237-241, 2011. [CrossRef] [Google Scholar] [Publisher Link]

[11] Holger Lange, "Automatic Glare Removal in Reflectance Imagery of the Uterine Cervix," *Medical Imaging 2005: Image Processing*, pp. 2183-2192, 2005. [CrossRef] [Google Scholar] [Publisher Link]

[12] V. Pallavi, and K. Payal, "Automated Analysis of Cervix Images to Grade the Severity of Cancer," *Annual International Conference of the IEEE Engineering in Medicine and Biology Society*, pp. 3439-3442, 2011. [CrossRef] [Google Scholar] [Publisher Link]

[13] Muhammad Asif et al., "Intrinsic Layer Based Automatic Specular Reflection Detection in Endoscopic Images," *Computers in Biology and Medicine*, vol. 128, no. 1, 2020. [CrossRef] [Google Scholar] [Publisher Link]

[14] Mojtaba Akbari et al., "Adaptive Specular Reflection Detection and Inpainting in Colonoscopy Video Frames," *25th IEEE International Conference on Image Processing*, pp. 3134-3138, 2018. [CrossRef] [Google Scholar] [Publisher Link]

[15] Leanne Attard et al., "Specular Highlights Detection Using a U-Net Based Deep Learning Architecture," *Fourth International Conference on Multimedia Computing, Networking and Applications*, pp. 4-6, 2020. [CrossRef] [Google Scholar] [Publisher Link]

[16] Yodit Abebe Ayalew, Kinde Anlay Fante, and Mohammed Aliy Mohammed, "Modified U-Net for Liver Cancer Segmentation from Computed Tomography Images with a New Class Balancing Method," *BMC Biomedical Engineering*, vol. 3, no. 4, pp. 1-13, 2021. [CrossRef] [Google Scholar] [Publisher Link]

[17] Juš Lozej et al., "End-to-End Iris Segmentation using U-Net," *IEEE International Work Conference on Bioinspired Intelligence,* pp. 1-6, 2018. [CrossRef] [Google Scholar] [Publisher Link]

[18] Bambang Krismono Triwijoyo, and Ahmat Adil, "Analysis of Medical Image Resizing using Bicubic Interpolation Algorithm," *Jurnal Ilmu Komputer*, vol. 14, no. 2, pp. 20-29, 2021. [Google Scholar] [Publisher Link]

[19] Olaf Ronneberger, Philipp Fischer, and Thomas Brox, "U-Net: Convolutional Networks for Biomedical Image Segmentation," *Medical Image Computing and Computer-Assisted Intervention-MICCAI 2015: 18th International Conference,* pp. 234-241, 2015. [CrossRef] [Google Scholar] [Publisher Link]

[20] Jonathan Long, Evan Shelhamer, and Trevor Darrell, "Fully Convolutional Networks for Semantic Segmentation," *IEEE Conference on Computer Vision and Pattern Recognition*, pp. 3431-3440, 2015. [Google Scholar] [Publisher Link]

[21] Baoxian Yu et al., "Specular Highlight Detection Based on Color Distribution for Endoscopic Images," *Frontier in Physics,* vol. 8, 2021. [CrossRef] [Google Scholar] [Publisher Link]

[22] Jian Yang Yefei Gao et al., "Dynamic Searching and Classification for Highlight Removal on Endoscopic Image," *Procedia of Computer Science,* vol. 107, no. 2017, pp. 762-767. [CrossRef] [Google Scholar] [Publisher Link]

[23] Kaggle, 2017. [Online]. Available: https://www.kaggle.com/competitions/intel-mobileodt-cervical-cancer-screening/overview/